Appl Phys A (2012) 109:789–796
DOI 10.1007/s00339-012-7346-z

Applied Physics A
Materials Science & Processing

High performance diffraction gratings made by e-beam lithography

Uwe D. Zeitner · Maria Oliva · Frank Fuchs · Dirk Michaelis · Tino Benkenstein · Torsten Harzendorf · Ernst-Bernhard Kley

Received: 22 February 2012 / Accepted: 10 October 2012 / Published online: 27 October 2012

Abstract Gratings are essential components in different high performance optical set-ups such as spectrometers in space missions or ultrashort-pulse laser compression arrangements. Often such kinds of applications require gratings operating close to the technological accessible limits of today's fabrication technology. Typical critical parameters are the diffraction efficiency and its polarization dependency, the wave-front error introduced by the grating, and the stray-light performance. Additionally, space applications have specific environmental requirements and laser application typically demand a high damage threshold. All these properties need to be controlled precisely on rather large grating areas. Grating sizes of 200 mm or even above are not unusual anymore. The paper provides a review on how such high performance gratings can be realized by electron-beam lithography and accompanying technologies. The approaches are demonstrated by different examples. The first example is the design and fabrication of the grating for the Radial-Velocity-Spectrometer of the GAIA-mission of the ESA. The second grating is a reflective pulse compression element with no wavelength resonances due to an optimized design. The last example shows a three level blazed grating in resonance domain with a diffraction efficiency of approximately 86 %.

U.D. Zeitner (✉) · M. Oliva · F. Fuchs · D. Michaelis · T. Benkenstein · T. Harzendorf
Fraunhofer Institute for Applied Optics & Precision Engineering, Albert-Einstein-Str. 7, 07745 Jena, Germany
e-mail: uwe.zeitner@iof.fraunhofer.de

U.D. Zeitner · E.-B. Kley
Institute for Applied Physics, Friedrich-Schiller-University Jena, Max Wien Platz 1, 07743 Jena, Germany

1 Introduction

Even about 200 years after the first grating spectrometer built by Joseph von Fraunhofer, exciting grating effects are still discovered and investigated. Diffraction gratings have not lost anything of their importance; they are key elements for a huge number of applications. The field of grating applications stretches from dispersing elements in spectrometers over beam-splitting elements to pulse-compression gratings for the manipulation of ultrashort laser pulses. The developments in modern lithographic fabrication technologies, especially the advances in resolution and accuracy of e-beam lithography, opened the way for the realization of subwavelength sized effective media structures. Exploiting this novel design freedom effective medium structures can be used beneficially in the realization of high performance diffraction gratings (see Fig. 1) for real applications.

In this paper, we will discuss the developed technology, based on electron beam lithography, used to fabricate such advanced diffraction gratings and show some examples.

2 Electron beam based technology

The core of our fabrication technology is the electron beam lithography process. The system installed at IOF Jena is a Vistec SB350 OS (Vistec Electron beam GmbH, Jena), which has been developed and specially adapted to requirements of optical applications. In fact, the letters OS stand for "optics special." The machine can handle substrate sizes up to an extension of 310 mm and 15 mm thickness, and achieves very high overlay accuracy and writing speed. The minimum feature size achievable is smaller than 50 nm, the address grid is 1 nm, and the overlay accuracy in case of a multiexposure process is better than 30 nm.

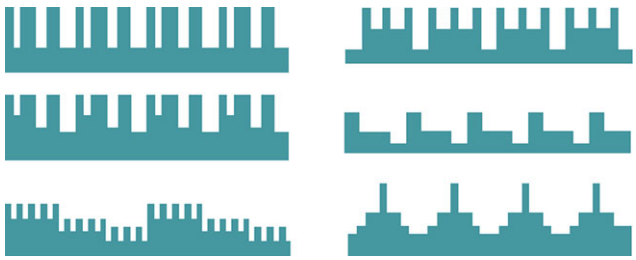

Fig. 1 Example profiles for the use of effective media structures in advanced diffraction gratings

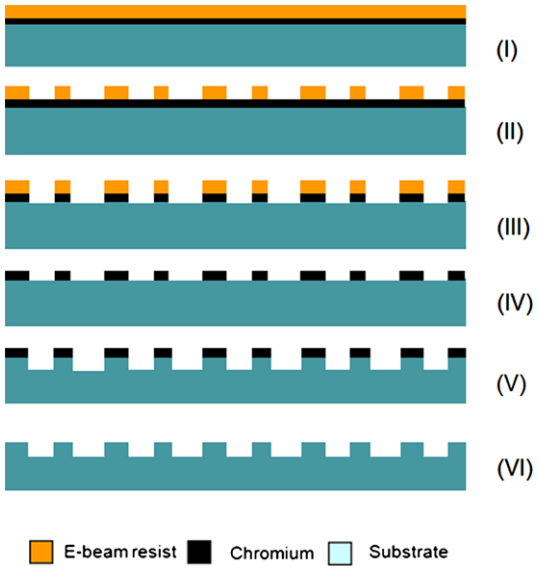

Fig. 2 Binary grating fabrication flow

The standard process flow for the fabrication of a binary optics structure is sketched in Fig. 2. The substrate, usually made of fused silica, is covered with an 80 nm thick chromium layer, on top of which an e-beam resist layer is coated (see Fig. 2(I)). The microstructure geometry is transferred to the resist by electron beam lithography and successive development of the exposed areas (see Fig. 2(II)). In the next step, the structured resist layer is used as a mask to transfer the pattern into the chromium layer by means of an RIE process (see Fig. 2(III)). After removing the resist, the patterned chromium layer serves as hard mask for the final deep etching into the substrate (see Fig. 2(IV–V)). Finally, the chromium layer is removed from the top of the grating.

To reduce the e-beam writing time, we use chemically amplified resists (CARs) like FEP171 (Fuji-Film). In the exposure data preparation, a structure dependent bias value is considered in order to account for the variation in the final lateral dimensions due to the different process steps.

To fabricate multilevel structures, the standard approach is to divide the desired profile into a combination of binary substructures, which are fabricated by repeated application of the above described binary fabrication process [1]. This approach becomes problematic with shrinking features size and periods of the structures, where the alignment errors between two exposures become more important. To overcome this problem, two different approaches for the fabrication of multilevel grating have been developed at Fraunhofer IOF. The first, named "three resist layer technology" is a simple modification of the standard approach. Here, after the etching of the first binary structure, an additional layer of conventional photoresist is used as a planarization for the chromium and resist coating of the second binary process step to aid the accurate patterning of the second layer [2]. In the second approach, the "relaxed alignment technology," a uniquely coded chromium mask (which contains all lateral pattern information) is used for all process steps in order to avoid alignment errors [3].

With the e-beam based technology described here several gratings, binary and multilevel, have been successfully fabricated. In the following, three examples will be described in detail.

3 High performance grating examples

The three different examples described in the following are high performance diffraction gratings with special requirements on design and technology. At first, the special design considerations and fabrication issues of a spectrometer grating for the space mission GAIA [4] is discussed. Secondly, in Sect. 3.2, we report about the design and fabrication of a reflection grating suppressing resonances by an optimized reflector design, suitable for spectroscopic or laser applications. Finally, a three-level grating in the resonance domain is discussed.

3.1 GAIA spectrometer grating

Specially tailored spectrometer gratings are required for many earth-observations or scientific space missions. The realization of such kinds of gratings is extremely demanding because multiple requirements have to be satisfied simultaneously. In particular, critical parameters are the diffraction efficiency and its polarization dependency, the wave-front error introduced by the grating, stray-light performance, and usability in a space environment. To achieve the optimal performance of the grating, it is essential to include technological considerations and specifications already into the design. We demonstrate this approach by the design and fabrication of the grating for the Radial-Velocity-Spectrometer (RVS) of the GAIA-mission of the European Space Agency (ESA). The corresponding instrument is dedicated to the measurement of the star distances for objects located in our home galaxy down to a relative brightness of $m = 18$ light magnitude. The distance measurement is based on a characterization of the red-shift of a calcium triple spectral line

Table 1 Required optical parameters of the spectrometer grating for the GAIA-Satellite of the ESA

Parameter	Value
Grating period	3.15 µm
Wavelength range	847 nm . . . 874 nm
Diffraction efficiency +1st order	>70 % (>77 % goal)
Polarization sensitivity $\frac{\lvert\eta_{TE}-\eta_{TM}\rvert}{\eta_{TE}+\eta_{TM}}$	<7 %
Angle of incidence	4.5°
Wave-front error	<5 nm (rms) on each 50 mm × 42 mm sub-aperture
Grating size	160 mm × 208 mm

group in the wavelength range $\lambda = 847 \ldots 874$ nm. In order to achieve the desired sensitivity, there is a combination of requirements to be fulfilled by the spectrometer grating, which makes it an extremely demanding optical element. An overview of the specification and requirements for the grating is given in Table 1.

Most of the requirements might be satisfied by gratings realized by any standard technology if they are considered alone, but their simultaneous implementation makes the fabrication extremely difficult. To achieve the blazing effect for a quasinormal incidence configuration, a linear phase modulation of the incident wave within one grating period is necessary. It is well known that this can be achieved by blazed gratings with a three-dimensional surface profile of the grating, i.e., a saw-tooth like structure or a stepwise approximation of it. However, the smaller the grating period, the more difficult the fabrication of such a 3D-structure becomes. For such small periods, typically the blazed profile can be approximated by a multilevel structure which can be fabricated by multiple succeeding binary patterning steps. However, if the alignment of the different lithography steps with respect to each other is not perfect the resulting structure can exhibit a considerable amount of stray-light, the diffraction efficiency is reduced, and also the quality of the transmitted wave-front is disturbed. As a result, the requirements mentioned in the above table will not be achieved with this technology, especially not on the whole grating area.

An alternative approach for the realization of efficient diffraction gratings is based on the modulation of the effective refractive index within the grating period by a binary subwavelength structure. This method of realizing highly efficient diffraction gratings by an effective index blaze has been experimentally demonstrated for instance by [5, 6].

The subwavelength features within the grating period are not resolved by the incident light, which instead is experiencing an effective refractive index averaged from the indices n_s and n_e of the substrate material and the environment (typically air), respectively. The particular effective index is a nontrivial function of the local fill-factor and typically also depends on the polarization of the light.

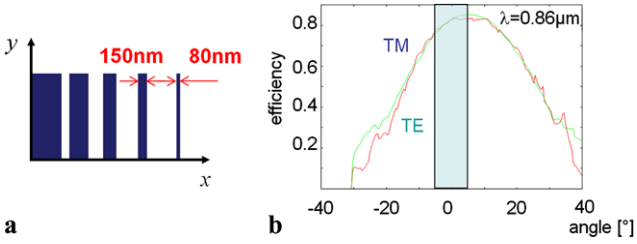

Fig. 3 GAIA spectrometer grating. (**a**) Optimized 1D effective medium structure. (**b**) Calculated diffraction efficiency as a function of the incidence angle for two orthogonal polarizations

From the technological point of view, the important advantage of this approach is the one step lithographic fabrication of the structure. There is no need for multiple successive and precisely aligned lithography steps as they would be required for the fabrication of multilevel profiles [1].

However, there is also a potential draw back of the effective index approach. The required aspect ratio, i.e., the ratio of structure depth to smallest feature width, is typically very high in such structures, especially if the grating is supposed to operate in the visible or near infrared spectral region. Then the required structures quickly approach the limits of the available fabrication technologies.

For the realization of the GAIA spectrometer grating, we thus developed an approach for the relaxation of the fabrication demands based on a combination of 1D and 2D subwavelength structures within one grating period. This particular example shall be used for the comparison of the relaxation potential of the transition from a pure 1D binary effective medium structure to a combination of 1D and 2D subwavelength features.

In a first grating design, we optimized a pure 1D binary blazed structure using a rigorous coupled wave algorithm (RCWA). The resulting structure, made of 5 bars within one grating period, is sketched in Fig. 3(a) together with a graph showing the angular dependency of the diffraction efficiency for TE- and TM-polarization at a wavelength of $\lambda = 860$ nm.

The required depth of the structure is $h = 1.83$ µm. As can be seen from the sketch, the smallest lateral bar width is 80 nm. Together with the required depth, this leads to an aspect ratio (structure height/width) of approximately 23, which is extremely difficult to fabricate.

In order to achieve a good homogeneity in the whole grating area, it is necessary to relax the demands on the fabrication process especially by reducing the high aspect ratio of the structures. We consider that for the optical function what is actually important is the local effective refractive index and this depends on the field overlap with the grating bars and grooves. Thus, the relevant parameter is the local filling factor and its variation across the grating period. Based on this idea, we extend the concept of the pure 1D grating structure to a 2D pattern. The smallest 1D bars have been replaced with 2D pillars, generating an additional

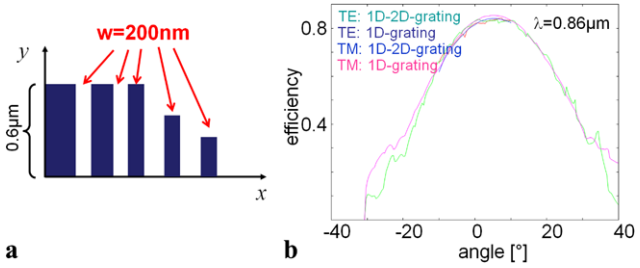

Fig. 4 GAIA spectrometer grating. (**a**) Optimized 1D–2D structure for the binary effective medium grating. (**b**) Comparison of the calculated diffraction efficiency of the two different grating types as a function of the incidence angle for two orthogonal polarizations

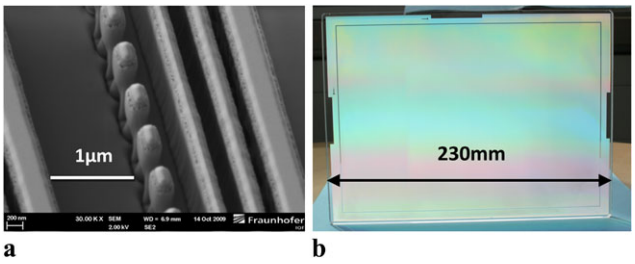

Fig. 5 GAIA spectrometer grating. (**a**) SEM-image of the fused silica grating structure fabricated by electron-beam lithography and reactive ion etching. (**b**) Photograph of the "Flight Model" of the grating

periodic structure along the y-direction of the grating having a sub-wavelength periodicity of $p_y = 600$ nm. Due to the sub-wavelength periodicity of this additional pattern in y-direction, it does not generate additional diffraction orders in this direction. By keeping the local fill-factor almost constant, this approach leads to 2D pillars instead of 1D bars with a considerably larger lateral feature size, thus being less demanding from a technological point of view. The resulting grating pattern is a combination of wide 1D bars and 2D pillars.

This combined 1D–2D pattern has been again optimized by a RCWA-algorithm with a constraint about the smallest lateral feature size of 200 nm (see Fig. 4). The structure depth of the optimized grating remains at about $h = 1.8$ µm. Thus, the aspect ratio is reduced from 23 in the pure 1D case to only 9 in the 1D–2D case leading to a much easier fabrication process. The optimized grating structure is shown in Fig. 4(a) together with a comparison of the efficiency performance of the two different grating types. It is clearly to be seen that the efficiency performance is similar to the pure 1D-grating but the minimum feature sizes are larger. The maximum theoretical efficiency for the incident angle of 4.5° is approximately 85 % for both polarization directions.

For the fabrication of the spectrometer grating, a combination of lithography and reactive ion etching (RIE) processes has been used as described in the Sect. 2 of this paper (see Fig. 2).

Achieving a high and polarization independent diffraction efficiency strongly depends on the accurate realization of the lateral features of the subwavelength pattern. If the bar width deviates from the design values, the efficiency for one of the polarization directions will increase or decrease. Therefore, an extensive optimization of the fabrication technology was necessary. First, a number of different grating designs were realized as gratings with a smaller size of only 30 mm × 30 mm in order to investigate how fabrication tolerances affect the achievable optical performance. From the different sample gratings, the most promising pattern geometry has been chosen for the realization of a full-size grating model. By including intermediate results from the technology optimization into a redesign of the grating structure made it possible to further simplify the grating structure without degrading the optical performance. As a result, the final grating pattern has a sub-structure within one grating period consisting of three 1D-bars and only one row of pillars, as shown in the SEM picture of Fig. 5(a). Their lateral feature sizes have been optimized in a close loop between the achieved experimental results and theoretical calculations, which considered also additional fabrication effects like the etch-depth dependence from the local groove width (the so called RIE-lag). One of the full-size "Flight Model" gratings fabricated at IOF is shown in Fig. 5(b).

For these gratings, specially polished 9″ sized substrates were used in order to obtain a wave-front error in the sub-apertures below 5 nm (rms) and a polarization independent diffraction efficiency above 80 %.

The measured efficiency, the polarization sensitivity, and the wave-front accuracy shown in Fig. 6 fulfill all the required specifications.

3.2 Resonance-free reflection gratings

The second type of grating that we discuss in this paper is an optimized reflection grating. Reflection gratings are preferable in several applications compared to the transmission ones due to the reduced material interaction and additional freedom for the optical design. Especially, the combination of gratings and dielectric mirrors are promising due to their low losses, and consequently high diffraction efficiencies. Using such a setup, almost 100 % diffraction efficiency can be achieved with a spectral bandwidth of several 10 nm or more and additional polarization-independency, depending on the specific setup. However, such kinds of multilayer dielectric gratings are challenged by the occurrence of guided mode resonances, which become noticeable as singular drops in the diffraction efficiency (cf. Fig. 7(a)).

The physical origin of the observed resonance features in the spectral response of the grating can be traced back to the excitation of guided modes in the dielectric layer stack used as reflector. Indeed, it is found that the coupling between the

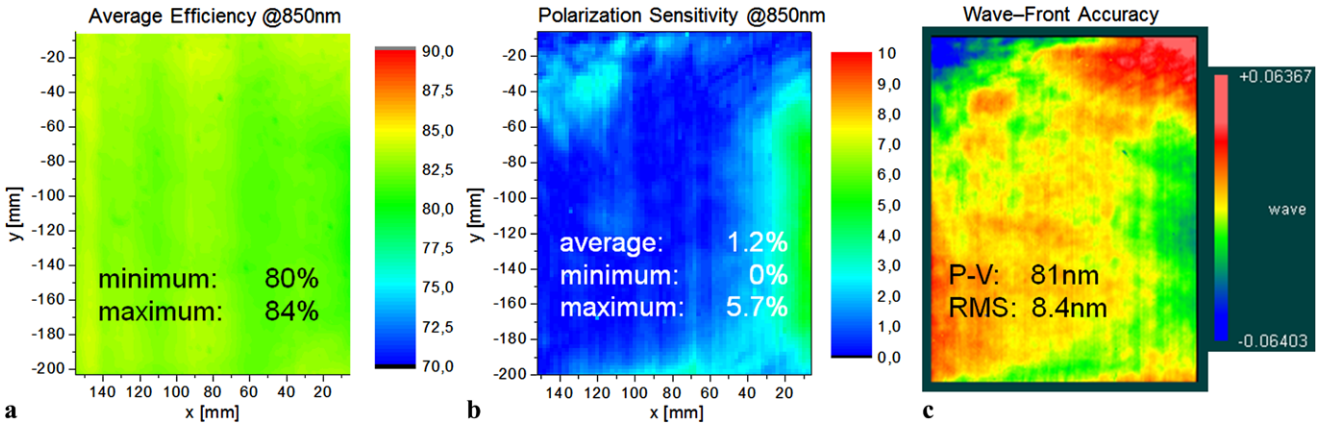

Fig. 6 GAIA spectrometer grating. (**a**) Average efficiency. (**b**) Polarization sensitivity. (**c**) Wave-front accuracy

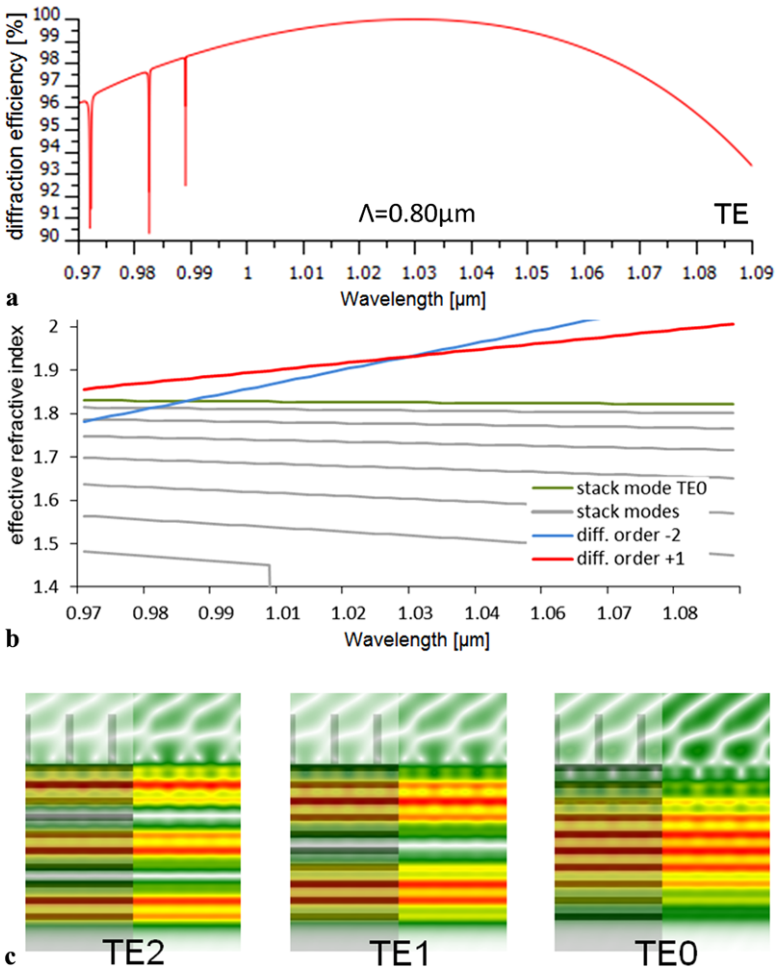

Fig. 7 (**a**) Diffraction efficiency for TE polarized light of a standard grating with 800 nm grating period and a regular reflector stack of $\lambda/4$ layers. The grating is illuminated at an incidence angle of 40.07° (Littrow angle for $\lambda = 1030$ nm). (**b**) Effective refractive indices (β_i / k_0) calculated for the modes of the stack-waveguide without grating. The corresponding excitation by the grating predicts the observed resonances. (**c**) Electrical field profiles calculated for the grating structure the resonant wavelengths. The field profile allows the common classification of the involved stack modes according to their nodal structure

modes of the grating and the waveguide is weak. Therefore, the resonant wavelengths can be predicted with high accuracy by the condition,

$$\beta_i = k_x^{\mathrm{inc}} + m\frac{2\pi}{\Lambda}, \tag{1}$$

where β_i is a guided mode of the dielectric stack (without grating), k_x^{inc} is the wave vector of the incident wave parallel to the interface, m is an integer labeling the diffraction orders of the grating, and Λ the grating period.

If the primary goal is either to avoid the formation of resonances, reduce their number in a certain spectral interval

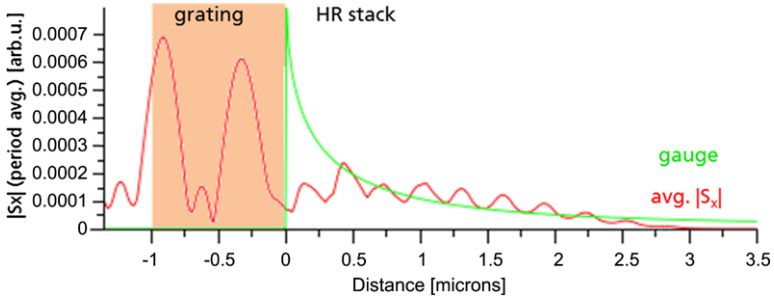

Fig. 8 Construction of the merit function. The averaged Poynting-vector component parallel to the interface is compared to a heuristically constructed gauge curve enforcing an exponential decay for the resonance-free case

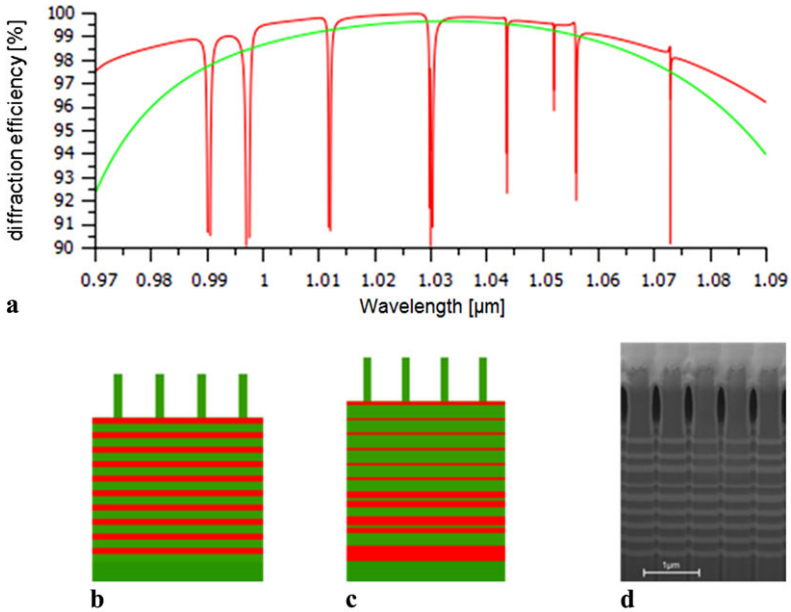

Fig. 9 (**a**) Diffraction efficiency for TE polarized light of a standard grating (*red curve* & design (**b**)) and a grating with the resonances removed (*green curve* & design (**c**)). Both gratings have a period of 875 nm and are illuminated at an incidence angle of 36.05° (Littrow angle for $\lambda = 1030$ nm). (**d**) FIB Cross-section of a fabricated reflection grating with aperiodic reflector-stack. The platinum layer visible on top of is needed for the focused ion beam cut process

or at least reduce their impact by quenching them below an acceptable width, knowing the resonant wavelengths is not enough. The only way to avoid resonances which can be directly derived from the resonance condition (1) is a significant reduction of the grating period, as suggested in [7]. However, such an approach is often found to be incompatible with the application requirements.

We, therefore, analyzed the formation of such guided mode resonances in dielectric reflection gratings in a little more detail to find a criterion for their evaluation and rating, such that this criterion can be directly used in the optimization of the grating structure. In order to be useful for the optimization, the rating criterion or merit function should especially provide a reasonable spectral width for the detection of resonances. For this reason, criteria based on the diffraction efficiency have been turned down early since the bandwidth of the resonances can vary quite drastically and especially become extremely narrow. Instead, we focused on the physical effects accompanying the formation of a resonance, more precisely on the characteristic enhancement of the electromagnetic fields (and derived quantities) inside the dielectric stack (cf. Fig. 7(c)). Different criteria (fields, energy density, and pointing vector) have been investigated. The most reliable way of identifying resonances has been found by using a merit function based on the analysis of the Poynting-vector inside the grating. It is based on the expectation that outside of a resonance the fields and the pointing vector should decay from the grating bottom into the stack. The merit function is constructed heuristically from the pointing vector component parallel to the interface. Practically, the overshoot of the computed Poynting-vector with respect to a parameterized exponential decay is measured for the detection and evaluation of the resonance (cf. Fig. 8). We tested this merit function successfully for the detection of resonances. The detection bandwidth is found to be a least one order of magnitude larger than the efficiency drop.

Using this merit function and going beyond the common design of a simple dielectric reflector formed by stacked double layers of $\lambda/4$ optical thicknesses, we exploit all structural degrees of freedom by a combined optimization of grating and layer stack. Indeed, the resonances can be removed successfully using this approach as shown in Fig. 9. In Fig. 9(b) and (c), the designs of a standard and resonance-free dielectric reflection grating are shown, respectively.

The aperiodicity of the layer stack is fundamental for the resonances elimination as it allows the tailoring of the stack

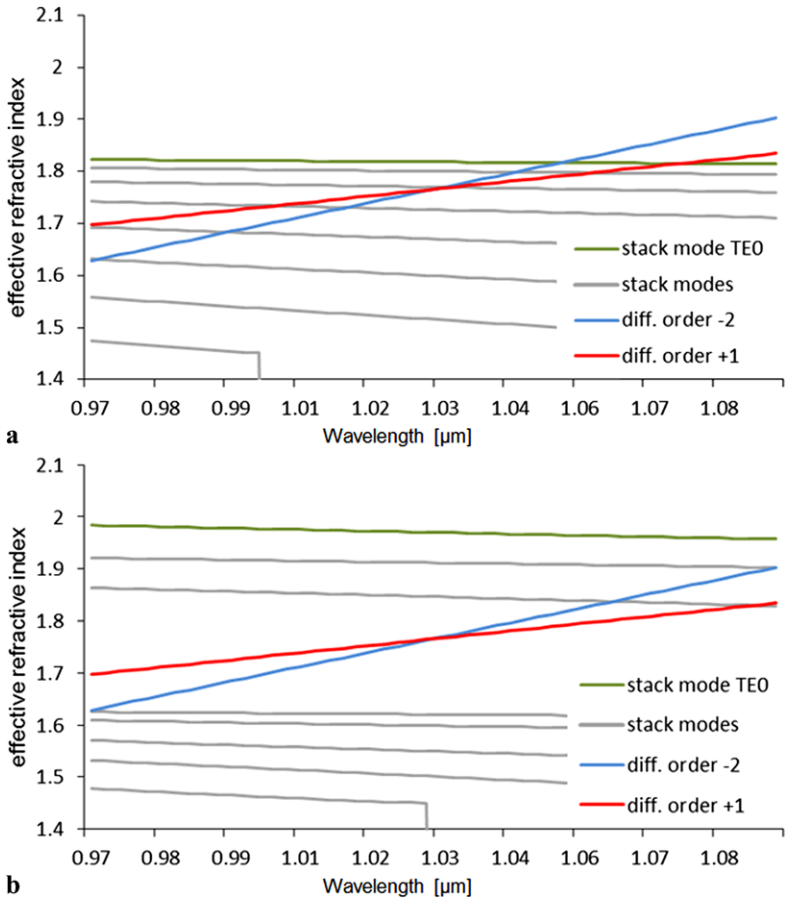

Fig. 10 (**a**) Effective refractive indices (β_i / k_0) and grating excitation calculated for a grating with a 875 nm period and a regular reflector stack as shown in Fig. 9(a). (**b**) As above, for an optimized aperiodic layer stack suppressing the guided mode resonances in the central wavelength interval

modes. Figure 10 shows the stack modes of the gratings structures in Fig. 9(b) and (c). It is obvious that the aperiodicity reduces the number excitable resonances by shifting the stack modes appropriately. Thereby, the grating efficiency is typically slightly reduced as can be seen in comparison of the red and green curves in Fig. 9(a).

Several resonance-free gratings, with different periods have been successfully fabricated by electron beam lithography and RIE etching into a silicon dioxide layer deposited on the top of the dielectric mirror layers. The FIB (Focused Ion Beam) image of Fig. 9(c) shows the profile of one of the fabricated grating profiles.

Such type of gratings having a period of $p = 667$ nm was successfully adapted for the NIR-spectrometer grating for the space mission Sentinel IV [8].

3.3 Highly efficient three level grating in resonance domain

The last grating presented here is a multilevel blazed grating working at normal incidence in resonance domain (small period-to-wavelength ratio). In such configurations, blazed gratings with a continuous profile as well as traditional multilevel gratings with equidistant phase levels show remarkable efficiency losses due to the shadowing effect [9]. The shadowing can be avoided using simple binary optical elements, but their single order efficiency at normal incidence is below 50 % due to symmetry reasons. To achieve a high efficiency at normal incidence, it is possible to perform a parametric optimization of the width and height of the different phase levels of a multilevel element [9]. We optimized the profile for a three-level grating in fused silica working at $\lambda = 633$ nm at normal incidence operating at the interface from substrate to air. The grating period $p = 1.266$ µm is two times the operating wavelength (633 nm). The optimized profile consists of an upper bar with a rather large height (∼778 nm) and a small width (200 nm) and a lower bar with moderate filling factor as well as aspect ratio (height ∼394 nm, width ∼580 nm). The high efficiency can be understood by a three-beam interference mechanism by considering the grating divided in two binary sub-gratings [2] both acting as beam splitting elements.

The three different technological approaches [10] already described for multilevel element fabrication have been tested for the fabrication of the grating in order to overcome inaccuracies and artifacts in the profile. The results of these fabrication tests have shown that all technologies are appropriate, but for the profile accuracy the most suitable approach is the “three-resist layer” technology.

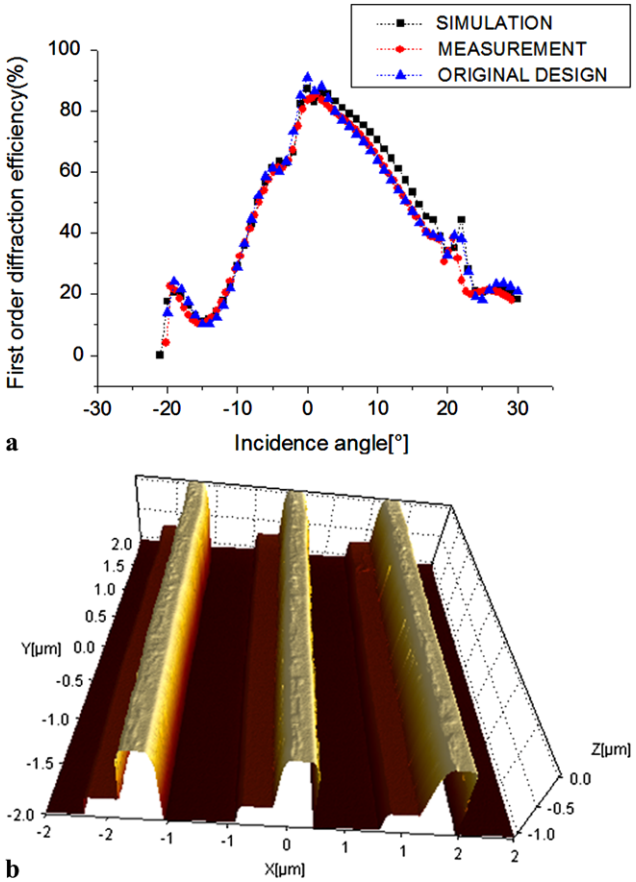

Fig. 11 Characterization of the grating. (**a**) Simulation and measurement of the 1st order diffraction efficiency vs. incidence angle. (**b**) AFM measurement of the three-level grating

In Fig. 11, the efficiency measurement and the AFM profile of a grating fabricated with this technological approach is shown. The measured diffraction efficiency of approximately 86 % at normal incidence is in very good agreement with the simulation as shown in Fig. 11(a). The atomic force microscopy measurement shows an almost perfect grating profile without any artifacts (see Fig. 11(b)) revealing that the proposed process is well suited for the fabrication of high quality resonance domain gratings.

4 Conclusions

Modern electron-beam lithography offers the required high accuracy, resolution, and especially a unique flexibility for the realization of high performance microstructured optical elements such as gratings for spaceborne spectrometers. Such applications often have a collection of extreme demands on the efficiency, polarization dependency, wavefront quality, stray-light level, and environmental conditions on the gratings. In order to fulfill all requirements at the same time novel grating concepts are necessary, which are not accessible by alternative grating fabrication technologies. In the current paper, we reported about the realization of three different types of gratings: (1) a binary-blazed transmission grating based on a subwavelength effective refractive index pattern for the spectrometer of the GAIA-satellite, (2) a resonance-free dielectric transmission grating for the Earth observation mission Sentinel IV, and (3) a three-level transmission grating in the resonance domain showing a high efficiency at normal incidence.

All examples do exhibit different unconventional grating features, which are hard to achieve by gratings realized by ruling or interference lithography due to lag of flexibility in shaping the grating profile with the required accuracy. These examples demonstrate the huge potential of electron beam lithography for the improvement of grating performance in different directions.

Acknowledgements The authors like to thank their colleagues from the CMN-Optics of the Fraunhofer IOF and the IAP of the FSU-Jena for their contributions to the realization of the gratings. All gratings exposures presented here were done using the e-beam writer SB350 OS at the Fraunhofer IOF whose purchase has been supported by the European Union (FZK: B 408—04004). Parts of the technology development presented here where supported by the German Ministry of Science and Education in the frame of the project PhoNa (FZK: 03IS2101D).

References

1. M.B. Stern, Binary optics fabrication, in *Microoptics: Elements, Systems, and Applications*, ed. by H.P. Herzig (Taylor & Francis, London, 1997)
2. M. Oliva, D. Michaelis, T. Benkenstein, J. Dunkel, T. Harzendorf, A. Matthes, U.D. Zeitner, Highly efficient three-level blazed grating in the resonance domain. Opt. Lett. **35**, 2774–2776 (2010)
3. M. Oliva, T. Harzendorf, D. Michaelis, U.D. Zeitner, A. Tünnermann, Multilevel blazed gratings in resonance domain: an alternative to the classical fabrication approach. Opt. Express **19**, 14735–14745 (2011)
4. www.gaia.esa.int
5. W. Stork, N. Streibl, H. Heidner, P. Kipfer, Artificial distributed-index media fabricated by zero-order gratings. Opt. Lett. **16**(24), 1921–1923 (1991)
6. P. Lalanne, S. Astilean, P. Chavel, E. Cambril, H. Launois, Blazed binary subwavelength gratings with efficiencies larger than those of conventional échelette gratings. Opt. Lett. **23**(14), 1081–1083 (1998)
7. J.-P. Wang, Y.-X. Jin, J.-Y. Ma, J.D. Shao, Z.-X. Fan, Analysis of restriction factors of widening diffraction bandwidth of multilayer dielectric grating. Chin. Phys. B **19**, 104201-8 (2010)
8. U.D. Zeitner, D. Michaelis, E.-B. Kley, M. Erdmann, High performance gratings for space applications. Proc. SPIE **7716**, 77161K (2010)
9. E. Noponen, J. Turunen, A. Vasara, Parametric optimization of multilevel diffractive optical elements by electromagnetic theory. Appl. Opt. **31**(28), 5910–5912 (1992)
10. M. Oliva, T. Benkenstein, J. Dunkel, T. Harzendorf, A. Matthes, D. Michaelis, U.D. Zeitner, Smart technology for blazed multilevel gratings in resonance domain. Proc. SPIE **7716**, 77161 (2010)